

UNCLASSIFIED

| |
|---|
| |
| |
| |
| AD NUMBER |
| AD008775 |
| NEW LIMITATION CHANGE |
| TO Approved for public release, distribution unlimited |
| FROM Distribution authorized to U.S. Gov't. agencies only; Foreign Government Information; MAR 1953. Other requests shall be referred to British Embassy, 3100 Massachusetts Avenue, NW, Washington, DC 20008. |
| AUTHORITY |
| DSTL, DEFE 15/511, 16 May 2008 |

THIS PAGE IS UNCLASSIFIED

Reproduced by

Armed Services Technical Information Agency
DOCUMENT SERVICE CENTER

KNOTT BUILDING, DAYTON, 2, OHIO

AD -

8775

UNCLASSIFIED

D No. 8775
OFFICE COPY



MINISTRY OF SUPPLY

ARMAMENT RESEARCH ESTABLISHMENT

REPORT No. 7/52

APPLIED MATHEMATICS & MECHANICS DIVISION

Wall Corrections to Axially
Symmetric Cavities in Circular Tunnels and Jets

A. H. Armstrong

K. G. Tadman

**THE INFORMATION IN THIS REPORT IS
DISCLOSED IN CONFIDENCE TO THE
RECIPIENT GOVERNMENT ON CONDITION
THAT IT IS NOT CIRCULATED OUTSIDE
GOVERNMENT DEPARTMENTS WITHOUT THE
PRIOR PERMISSION OF THE MINISTRY OF
SUPPLY.**

UNCLASSIFIED

Ministry of Supply

ARMAMENT RESEARCH ESTABLISHMENT

REPORT NO. 7/52

(Theoretical Research Report No. 1/52)

Wall corrections to axially symmetric cavities in circular
tunnels and jets.

A. H. Armstrong and K. G. Tadman

Summary

Using the fact that cavities are, at low cavitation numbers, approximately prolate spheroids, this report develops the theory of wall corrections in closed tunnels and free jets of circular cross-section.

The results are displayed graphically for a wide range of the ratio (cavity length) / (tunnel width).

In addition, a first-order theory is developed which applies only to small cavities at low cavitation numbers. The wall correction is then shown to be proportional to the cube of this ratio, whereas in two-dimensional theory it is proportional to the square of the ratio. Moreover, the corrections in a closed tunnel are shown to be roughly four times as great as, and in the opposite sense to, those applicable to free jets. In two-dimensional theory they are twice as great.

The unaided theory yields information on the thickness ratio only of the cavity. However, if the additional assumption is made that the drag coefficient is relatively insensitive to boundary effects - an assumption which is certainly true for the two-dimensional case - than the length and breadth of the cavity may be investigated separately. It is thus found that, in the axisymmetric as in the two-dimensional case, the boundary correction to the length of a small cavity is proportionately twice as great as that to the width.

Approved

..... *J. Marshall* Senior Superintendent.

UNCLASSIFIED

IMPORTANT

This DOCUMENT should be returned to the Chief Information Officer, Armament Research Establishment, Fort Halstead, Sevenoaks, Kent, if retention becomes no longer necessary.

INITIAL DISTRIBUTION

Internal

No. 1 CSAR
2 SSAM
3 STA
4-5 STA (Att. Mr. A.H. Armstrong, Mr. K.G. Tadman)
6-7 AM Records

United Kingdom

8-9 CS/ERDE
10 DWR(D)

11 ACSIL
12 ATDU (Att. Mr. L.W. Parkin)
13 CEAD (Att. Dr. M. Simmons)
14 College of Aeronautics (Att. Librarian)
15 DAER
16 DFR
17 DRAE (Att. Mr. Duncan)
18 DUW
19 MAEE
20 Secretary OB
21 Superintendent AHBRE
22-24 Superintendent ARL (Att. Mr. Burt, Mr. Campbell, Mr. Craig)
25 UCWE

Overseas (through TPA3/TIB)

26-43 US - Joint Reading Panel
44 - R and D Board
45 - Director, Maths. Div., Office of Naval Research,
Washington D.C. (Att. Dr. M. Rees)
46 - Commander, Underwater Ord. Div., Naval Ord Test Station,
Pasadena, California. (Att. Dr. J.G. Waugh)
47-48 - Director, David W. Taylor Model Basin, Washington D.C.
(Att. Dr. E.H. Kennard, Dr. P. Eisenberg)
49-50 - Hydrodynamics Laboratory, California Institute
of Technology, Pasadena, California.
(Att. Dr. R.T. Knapp, Dr. M.S. Plesset)
51-52 - Director, Experimental Towing Tank, Stevens Institute
of Technology, Hoboken N.J.
(Att. Dr. K.S.M. Davidson, Dr. B.V. Korvin-Kroukovsky)
53 - Dr. L.G. Straub, Director, St. Anthony Falls Hydraulic
Lab. Univ. of Minnesota, Minneapolis, Minnesota.
54 - Dr. Hunter Rouse, Iowa Inst. of Hydraulic Research
State University of Iowa, Iowa City, Iowa.
55 - Prof. G. Birkhoff, Indiana Univ., Bloomington, Indiana.
56 - Dr. J. Serrin, Princeton Univ., Princeton, N.J.

57-60 BJSB (incl. Naval Staff) for own use only.

61 Canada - Dept. Nat. Def.
62-65 - Def. Res. Liaison
66 - Nat. Res. Council

67-68 TPA3/TIB - Retention

| <u>Contents</u> | <u>Page</u> |
|---|-------------|
| Symbols | 1 |
| Introduction | 4 |
| 1. Notation. | 5 |
| 2. Cavity in an unbounded stream. | 6 |
| 3. Cavity in a stream of circular cross-section. | 7 |
| 4. First-order theory for two-dimensional cavities. | 10 |
| (a) Closed tunnel | 10 |
| (b) Free jet. | 13 |
| 5. First-order theory for axially symmetric cavities. | 17 |
| 6. Use of the drag coefficients to determine cavity dimensions. | 19 |
| 7. Numerical results. | 22 |
| 8. Conclusions. | 24 |
| References. | 26 |
| Appendix I | 27 |
| Appendix II | 29 |

Symbols

Roman letters

| | |
|----------------|--|
| A, B | auxiliary functions defined in equations (7.1). |
| c | the radius or semi-width of the cavitating head. |
| $C_0(\kappa')$ | an auxiliary function of κ' used in equation (4.14). |
| C_D | the true drag coefficient, based on the area of cross-section of the cavitating head. |
| C_D' | the modified drag coefficient, based on the area of cross-section of the cavity. |
| $C_{\nu, n}$ | coefficients defined in Appendix II. |
| $D_0(\kappa')$ | an auxiliary function of κ' used in equation (4.14). |
| E, E' | incomplete elliptic integrals defined in equation (4.5). |
| f | the semi-length of the distribution of sources and sinks on the axis. |
| F, F' | incomplete elliptic integrals defined in equation (4.5). |
| $g(\delta)$ | an auxiliary function defined in equation (4.2). |
| G | a function relating the cavitation number to the size of the cavity. |
| $I(\mu_0)$ | an auxiliary function defined in equation (6.3). |
| J_ν | the Bessel function of the first kind and of order ν . |
| k, k' | the modulus and co-modulus of elliptic integrals defined in equation (4.4). Physically, k' provides a rough measure of the cavitation number. |
| $k_{\nu, m}$ | the m th. positive zero of $J_\nu(z)$, taken in ascending numerical order. |
| K | a complete elliptic integral defined in equation (4.5). |
| m | mU is the axial component of fluid velocity. |
| m_0 | the particular value of m at the equator of the cavity. |
| M | a function relating the strength of the uniform stream to the size of the cavity. |
| p | a parameter occurring in equation (3.2). |
| P_0 | the uniform pressure along the cavity wall. |
| P_∞ | the pressure in the undisturbed stream, far from the cavity. |
| q | a mathematical parameter introduced in equations (4.14). Physically, it provides a rough measure of the ratio of the size of the cavity to the diameter of the stream. |
| Q | cavitation number. |

- μ_{∞} = $G (\mu_{\infty})$, the cavitation number in the unbounded stream which would yield a cavity of the length actually observed in the bounded stream.
- μ_0 = $G (\mu_0)$, the cavitation number in the unbounded stream, which would yield a cavity of the width actually observed in the bounded stream.
- R denotes a remainder term of smaller order than the terms retained.
- t a variable of summation.
- u a variable of integration.
- V velocity of the undisturbed stream.
- x non-dimensional coordinate parallel to axis of symmetry } unit of length is radius of tunnel
- y non-dimensional coordinate perpendicular to axis of symmetry }
- x_0 the semi-length of the cavity.
- r_0 the equatorial radius or semi-width of the cavity.
- $X_i(\kappa')$ } auxiliary functions of κ' used in equations (4.14).
- $Y_i(\kappa')$ }

Greek Letters

- $\Gamma_1, \Gamma_2, \Gamma_3$ auxiliary functions of q , defined in equations (4.17).
- δ a mathematical parameter introduced by equations (4.1). Physically, it provides a rough measure of the ratio of the size of the cavity to the diameter of the stream.
- Δ an operator indicating the difference between a bounded stream value and the corresponding unbounded stream value.
- $\Delta_1, \Delta_2, \Delta_3, \Delta_4$ terms contributing to $\Delta I (\mu_0)$.
- ϵ the displacement of the jet surface at the plane of symmetry.
- κ' a mathematical parameter defined in equation (4.15). Physically, it is a function of the cavitation number only.
- λ, μ conicoidal coordinates defined by equation (1.1).
- μ_0, μ_{∞} particular values of μ at the equator and pole of the cavity, respectively.
- ν a parameter taking the value 0 for a free surface and 1 for a fixed boundary.
- ξ the x -coordinate of a source element.

- ρ density of the liquid.
- $\phi_a(x, y)$ that part of the axial component of velocity contributed by the line source-sink.
- $\phi(x, y, \nu, p)$ a potential function defined in equation (3.9).
- $\psi(x, y)$ Stokes' stream function.
- $\Omega(x, y)$ a current function defined in equation (1.5).
- $\Omega_a(x, y)$ that part of the current function contributed by the line source-sink.
- $\Omega(x, y, \nu, p)$ a particular current function defined in equation (3.2).

A bar indicates that the symbols apply to the unbounded stream.

UNCLASSIFIED

Introduction

The purpose of this report is to investigate wall effects on the overall proportions of a cavity formed by an axially symmetric body in rapid motion relative to a stream of water. In the laboratory it is possible to measure the dimensions of such a cavity, formed in a stream having a certain finite cross-sectional area. The problem then is to calculate what the dimensions would be if such a cavity were formed in a stream of unlimited extent in all directions.

There already exists a considerable literature on the theory of wall corrections applicable to non-cavitating flow in wind- or water-tunnels. In that case, however, the boundaries of the flow are determined, being the walls of the tunnel and the surface of the aerodynamic body under test, and the problem consists of determining the corrections to be applied to the velocity or pressure field. In our case, on the other hand, the internal boundary of the flow is variable, being the surface of the cavity, and only the pressure distribution along it is known.

In two dimensions, the problem has been solved for certain simple head shapes by the use of conformal transformations (ref. 1 and 6). In three dimensions, even under the assumption of axial symmetry, this powerful method is no longer available. A partial and approximate solution of the axially symmetric problem will, however, be derived in the following pages by the use of source-sink methods.

The basic fact underlying our present method is that the shapes of such cavities are known to approximate to prolate spheroids. Furthermore, it is possible to produce closed stream surfaces, which are either exactly or approximately spheroidal in shape, by combining a very simple axial source-sink distribution with a uniform stream of either unbounded or bounded extent, respectively.

The characteristic feature of cavity flow is, of course, that the fluid pressure is uniform along the free surface of the cavity, and a dimensionless cavitation number, Q , is accordingly defined by the ratio

$$Q = \frac{P_{\infty} - P_c}{\frac{1}{2} \rho U^2} \quad (0.1)$$

Here P_{∞} and P_c are pressure in the undisturbed stream and the pressure on the cavity wall respectively, whilst ρ and U are the density of the liquid and the velocity of the undisturbed stream.

In the flow-patterns which we shall construct by source-sink methods, the pressure along the closed stream surface will be only approximately uniform, this constituting an intrinsic imperfection of the method, and we shall adopt the convention of considering the pressure at the equator of the stream-surface as characteristic of the "cavity". The cavitation number will then be defined in terms of this equatorial pressure.

Without any further assumptions we can then investigate the effect of the boundary on the thickness ratio of the cavity, at a given cavitation number. In order to investigate the behaviour of the length and width separately, however, we make the assumption, rendered plausible by the known results of two-dimensional theory, that the drag coefficient of a small cavity is unaffected, to a high degree of accuracy, by the boundary.

1. Notation

In this report it will be convenient to employ two non-dimensional coordinate systems, and the necessary transformations are set out here for ease of reference. The cylindrical coordinate system (Fig. 1) will employ x , measured along the axis of symmetry from the centre of the cavity, and y , measured perpendicularly from the axis of symmetry. The conicoidal coordinate system (Fig. 2) will employ λ , which is constant on each member of a confocal system of hyperboloids of revolution, and μ , which is constant on each member of the orthogonal system of confocal prolate spheroids. The foci of this system are at $y = 0$, $x = \pm f$, where f is a positive parameter. The relations between (x, y) and (λ, μ) are

$$\left. \begin{aligned} x/f &= \tanh \lambda \coth \mu \\ y/f &= \operatorname{sech} \lambda \operatorname{cosech} \mu \end{aligned} \right\} \quad (1.1)$$

and, in particular,

$$\left. \begin{aligned} \text{when } x &= 0 & \lambda &= 0, \\ \text{when } y &= 0 \ (|x| > f) & \lambda &= \pm \pi, \\ \text{when } y &= 0 \ (|x| < f) & \mu &= \infty. \end{aligned} \right\} \quad (1.2)$$

We shall study the shape of the closed stream-surface generated by the superposition of a uniform stream of velocity U , parallel to the x -axis, on a certain source-sink distribution. The latter extends along the x -axis from $-f$ to $+f$ and has a density equal to x . The unit of length is the radius of the stream at infinity, so that the limiting case of an unbounded stream is obtained by letting f tend to zero. The fineness ratio of the closed stream-surface is controlled by the choice of U .

The semi-length of the closed stream-surface, that is, the value of x when $y = 0$, will be denoted by x_0 . Similarly, the equatorial radius of the closed stream surface, that is, the value of y when $x = 0$, will be denoted by y_0 . On the same basis, the value of μ at $x = 0$, $y = y_0$, will be denoted by μ_0 , and the value of μ at $x = x_0$, $y = 0$, will be denoted by μ_∞ . Thus

$$\left. \begin{aligned} y_0/f &= \operatorname{cosech} \mu_0 \\ x_0/f &= \coth \mu_\infty \end{aligned} \right\} \quad (1.3)$$

The results of the analysis will be displayed in the form of a comparison between the properties of the closed stream surface for general values of f with the corresponding properties in the limiting case of the unbounded stream. Accordingly, it will be convenient to use a bar to indicate values applying to the case of the unbounded stream, and the symbol Δ to indicate the difference between the value for the bounded stream and that for the unbounded stream. Thus, for example,

$$U = \bar{U} + \Delta U \quad (1.4)$$

It is usual to describe axisymmetric flow patterns by means of Stokes' stream function $\psi(x, y)$, where $2\pi\psi(x, y)$ is the rate of volume flow of liquid through the circle (x, y) in the positive direction of x . Because, however, this function vanishes identically on the axis of symmetry, it will be more convenient here to use a current function $\Omega(x, y)$ defined by

$$y^2 \Omega(x, y) = \psi(x, y) \quad (1.5)$$

This function has an obvious physical significance, for it is equal to half the average x -component of velocity inside the circle (x, y) . It vanishes on the x -axis only at special points, namely the stagnation points $(\pm x_0, 0)$.

The closed stream surface $\psi(x,y) = 0$ breaks up into two branches, namely the axis of symmetry $y = 0$ and the closed stream surface $\Omega(x,y) = 0$. It is only the latter branch which is of interest in this paper.

From this point onwards, in the interests of brevity, we shall replace the strictly correct appellation "closed stream surface" by the rather loose term "cavity".

The axial component of the fluid velocity at any point of the flow will be denoted by mU , so that m is a function of x and y , or of λ and μ . In practice, however, we shall only study the variation of m in the plane $x = 0$, where, by symmetry, mU is the actual magnitude of velocity. The particular value of m at the equator of the cavity will be denoted by m_0 , and it follows easily from Bernoulli's law, and the definition (0.1) of the cavitation number, that

$$1 + Q = m_0^2 . \quad (1.6)$$

It is often convenient in cavitation theory to consider two drag coefficients, the first, C_D , being based on the area of the plate which is supposed to be causing the cavity; and the second, C_D' , being based on the maximum cross-sectional area of the cavity. It will be convenient to distinguish between the two by referring to them in this report as the "true" and the "modified" drag coefficient, respectively. If the radius of the cavitating plate is denoted by c , then we have the obvious relationship

$$y_0^2/c^2 = C_D/C_D' . \quad (1.7)$$

Simmons (ref. 1) has shown, from considerations of momentum and continuity, that

$$C_D' = Q - 2y_0^2 \int_{y_0}^1 (m-1)^2 y \, dy , \quad (1.8)$$

the integral being evaluated along the y axis ($x = 0$). It will be possible to calculate the boundary effect on C_D' , and hence, by making a plausible assumption as to the behaviour of C_D , it will be possible to deduce the boundary effect on the ratio y_0/c from equation (1.7).

2. Cavity in an unbounded stream

We develop first the theory for the unbounded stream, as the analysis required is simpler than, and completely dissimilar from, that required for the stream of finite lateral extent. The fact that this case corresponds to a vanishingly small value of f is no inconvenience, since all the ratios of length which occur in this section are finite in size.

The current function $\bar{\Omega}(x,y)$ of the flow pattern is given by

$$2\bar{\Omega}(x,y) = \bar{U} + \int_{-f}^f \frac{(x-\xi) d\xi}{y^2 \{y^2 + (x-\xi)^2\}^{1/2}} . \quad (2.1)$$

After transformation to the conicoidal coordinates (λ, μ) this is easily integrated to give

$$2\bar{\Omega}(x,y) = \bar{U} - \left(\frac{1}{2}\right) \sinh 2\mu - \mu . \quad (2.2)$$

The cavity surface $\bar{\Omega}(x,y) = 0$ is thus the prolate spheroid $\mu = \bar{U}_0$ where

$$\bar{U} = M(\bar{\mu}_0) = \frac{1}{2} \sinh 2\bar{\mu}_0 - \bar{\mu}_0, \quad (2.3)$$

and

$$\bar{\mu}_0 = \bar{\mu}_\infty. \quad (2.4)$$

The axial component of velocity is given by the equation

$$\bar{m} \bar{U} = \frac{1}{y} \frac{\partial \bar{\psi}}{\partial y} = 2\bar{\eta} + y \frac{\partial \bar{\eta}}{\partial y}. \quad (2.5)$$

In the plane of symmetry, where $\lambda = 0$ it follows from (1.1) that the operator $(y d/dy)$ is equivalent to the operator $(-\tanh \mu d/d\mu)$, so that the substitution of (2.2) in (2.5) yields eventually

$$(\bar{m} - 1) \bar{U} = \mu - \tanh \mu, \quad (\lambda = 0). \quad (2.6)$$

Hence, using the relation (1.6), we obtain for the cavitation number the expression

$$\bar{Q} = G(\bar{\mu}_0) = \left[\frac{\tanh \bar{\mu}_0 \sinh^2 \bar{\mu}_0}{\sinh \bar{\mu}_0 \cosh \bar{\mu}_0 - \bar{\mu}_0} \right]^2 - 1. \quad (2.7)$$

The dimensions of the cavity are obtained immediately from (1.3), thus

$$\text{and } \left. \begin{aligned} \bar{y}_0/f &= \operatorname{cosech} \bar{\mu}_0 \\ \bar{x}_0/f &= \operatorname{coth} \bar{\mu}_0. \end{aligned} \right\} \quad (2.8)$$

Moreover, on substituting (2.6) and (2.7) into (1.8) and evaluating the integral, we find that

$$\bar{U} \bar{C}_D' = \sinh^2 \bar{\mu}_0 (\ln \cosh^2 \bar{\mu}_0 - \tanh^2 \bar{\mu}_0). \quad (2.9)$$

3. Cavity in a stream of circular cross-section

In the previous section we examined the flow patterns produced by a linear distribution of sources and sinks immersed in an otherwise uniform unbounded stream. The object of this section will be to examine the flow patterns produced by the same line source-sink immersed in a stream which has a finite circular cross-section. It is convenient to take the radius of the cross-section of the undisturbed stream as unity, so that certain boundary conditions have to be satisfied on the cylinder $y = 1$.

We shall consider two cases, firstly when the stream is enclosed by a rigid cylindrical wall, and secondly when it is open on all sides to an atmosphere at constant pressure. The first case obviously imposes the boundary condition

that the cylinder $y = 1$ shall be a stream surface, in other words $\Omega(x,1) = \text{constant}$. Moreover, consideration of conditions far upstream or downstream of the cavity shows that the constant is simply $\frac{1}{2} U$.

In the second case the mathematical boundary condition only approximates to the physical boundary conditions. For, instead of ensuring that the velocity magnitude shall be constant on the disturbed free surface, we actually stipulate that the axial component of velocity shall be constant on the cylinder $y = 1$. The validity of this approximation has been investigated in Appendix I, where it is shown that the errors involved are not serious in that part of the field which forms the subject of this report.

The current function due to a unit point source situated at $(\xi, 0)$ inside a free or fixed cylindrical boundary, having the equation $y = 1$, is given by (ref. 2,3)

$$\left. \begin{aligned} & -\frac{1}{2}\nu + \Omega(x-\xi, y, \nu, -1) \quad \text{when } x > \xi \\ \text{or} \quad & \frac{1}{2}\nu - y^{-2} - \Omega(\xi-x, y, \nu, -1) \quad \text{when } x < \xi. \end{aligned} \right\} (3.1)$$

Here

$$\Omega(x, y, \nu, p) = \sum_{m=1}^{\infty} (-k_{\nu, m})^p \frac{J_1(k_{\nu, m} y)}{y J_{1-\nu}(k_{\nu, m})} \exp(-k_{\nu, m} x), \quad (3.2)$$

$k_{\nu, m}$ is the m th. positive zero of $J_{\nu}(z)$, and $\nu = 0$ for a free boundary and $\nu = 1$ for a fixed boundary.

On integrating from $\xi = -f$ to $\xi = f$, to obtain the current function $\Omega_0(x, y)$ due to the line source-sink, the result takes different analytical forms according to the relative magnitudes of x and f . The two essentially different cases are as follows:

(i)

When $0 < x < f$,

$$\begin{aligned} \Omega_0(x, y) &= \int_{-f}^x \left\{ -\frac{1}{2}\nu + \Omega(x-\xi, y, \nu, -1) \right\} \xi \, d\xi + \int_x^f \left\{ \frac{1}{2}\nu - y^{-2} - \Omega(\xi-x, y, \nu, -1) \right\} \xi \, d\xi \\ &= \left[\xi \Omega(x-\xi, y, \nu, -2) + \Omega(x-\xi, y, \nu, -3) \right]_x^{-f} + \frac{1}{2} \nu (f^2 - x^2) \\ &+ \left[\xi \Omega(\xi-x, y, \nu, -2) - \Omega(\xi-x, y, \nu, -3) + \frac{1}{2} \xi^2 / y^2 \right]_f^x. \end{aligned} \quad (3.3)$$

(ii)

When $f < x$

$$\begin{aligned} \Omega_0(x, y) &= \int_{-f}^f \left\{ -\frac{1}{2}\nu + \Omega(x-\xi, y, \nu, -1) \right\} \xi \, d\xi \\ &= \left[\xi \Omega(x-\xi, y, \nu, -2) + \Omega(x-\xi, y, \nu, -3) \right]_f^{-f} \end{aligned} \quad (3.4)$$

The current function of the combined flow pattern, $\Omega(x, y)$, is simply the sum of the current function due to the line source-sink, $\Omega_0(x, y)$,

and that due to the uniform stream: thus

$$\Omega(x,y) = \frac{1}{2} U + \Omega_g(x,y) . \quad (3.5)$$

The function $\Omega_g(x,y)$ is the sum of an infinite series of products of Bessel functions and exponential functions, but, by means of certain transformations listed in Appendix II, it can be expressed in another form. Thus,

$$2\Omega_g(x,y) = -\left(\frac{1}{8} \sinh 2\mu - \mu\right) + \sum_{s} C_{s,s} f^s + R(x,y,f) , \quad (3.6)$$

where $C_{s,s}$ are constants and $R(x,y,f)$ is the sum of an infinite series whose n th. term is a homogeneous polynomial in x, y and f of degree $(n+3)$. This form demonstrates the similarity between the current function for unbounded flow (2.2) and that for bounded flow (3.5), and will be particularly useful in a later section for developing a first order theory for small cavities.

The equation of the closed stream surface may now be obtained by equating $\Omega(x,y)$ to zero. The resulting functional relation between x and y is rather complex, but we shall investigate only the overall dimensions of the cavity, namely x_0 and y_0 . These quantities - the semi-length and equatorial radius of the cavity, respectively - are given by the equations

$$\Omega(x_0, 0) = 0 \text{ and } \Omega(0, y_0) = 0 . \quad (3.7)$$

Next, it is necessary to differentiate $y^2 \Omega(x,y)$ partially with respect to y , in order to obtain the axial velocity component $m U$. We observe that

$$-\frac{1}{y} \frac{\partial}{\partial y} \left\{ y^2 \Omega(x,y, \nu, p) \right\} = \phi(x,y, \nu, p+1) , \quad (3.8)$$

where

$$\phi(x,y, \nu, p) = \sum_{m=1}^{\infty} (-k_{\nu, m})^p \frac{J_0(k_{\nu, m} y)}{J_{1-\nu}^2(k_{\nu, m})} \exp(-k_{\nu, m} x) . \quad (3.9)$$

It follows from (3.5) that

$$mU = \frac{1}{y} \frac{\partial}{\partial y} \left\{ y^2 \Omega(x,y) \right\} = U - \phi_g(x,y) , \quad (3.10)$$

where

$$\left. \begin{aligned} \phi_g(x,y) &= \left[\xi \phi(x-\xi, y, \nu, -1) + \phi(x-\xi, y, \nu, -2) \right]_x^{-f} - \nu(f^2 - x^2) \\ &+ \left[\xi \phi(\xi - x, y, \nu, -1) - \phi(\xi - x, y, \nu, -2) \right]_f^x \quad (0 < x < f) \\ \text{or} \\ &= \left[\xi \phi(x-\xi, y, \nu, -1) + \phi(x-\xi, y, \nu, -2) \right]_f^{-f} \quad (f < x) . \end{aligned} \right\} \quad (3.11)$$

On making use of the transformations given in Appendix II, one can express (3.10) in the form

$$(m-1) U = \mu - \frac{1}{2} \cosh \lambda \sinh \mu \{ \operatorname{sech}(\lambda + \mu) + \operatorname{sech}(\lambda - \mu) \} + \frac{1}{2} C_{\nu, s} r^2 + R(x, y, r); \quad (3.12)$$

alternatively, this expression may be obtained directly from (3.6).

In particular, at the equatorial plane x and λ vanish, so that, from (3.10, 11, 12,)

$$(m-1) U = \left. \begin{aligned} & 2f \phi(f, y, \nu, -1) - 2\phi(f, y, \nu, -2) + 2\phi(0, y, \nu, -2) + \nu r^2 \\ & = \mu - \tanh \mu + \frac{1}{2} C_{\nu, s} r^2 + R(0, y, r), \end{aligned} \right\} (\lambda=0) \quad (3.13)$$

and the corresponding formula for m_0 is obtained by simply adding the suffix zero to the symbols m , y and μ . Finally, Q follows from equation (1.6), and (1.8) then yields C_D^2 after a numerical integration.

4. First order theory for two-dimensional cavities

Before developing a first order theory for axially symmetric cavities it seems advisable to set on record the corresponding results for two-dimensional cavities behind a flat plate. The exact mathematical theory of a two-dimensional cavity behind a flat plate in a bounded open or closed stream has been developed by Simmons (ref. 1), but a certain amount of algebraic manipulation is necessary in order to extract the results which we require.

(a) Closed tunnel

A suitable starting point for developing a first order theory in the case of the closed tunnel is furnished by Simmon's equations (47, 54, 56 and 62) (ref. 1). In the present notation, these become:

$$\left. \begin{aligned} \frac{1}{2} km_0 v_0 &= g(\delta) + k' \sec \delta \tan^{-1}(k' \tan \delta), \\ \frac{1}{2} km_0 w_0 &= k^2 K \sin \delta - \sec \delta (1 - k^2 \sin^2 \delta)^{1/2} [K E(\delta) - E F(\delta)], \\ \frac{1}{2} km_0 y_0 &= g(\delta) + k' \delta \sec \delta, \\ k v_0 C_D / 4 m_0 &= g(\delta), \end{aligned} \right\} \quad (4.1)$$

where

$$g(\delta) = \sec \delta (1 - k^2 \sin^2 \delta)^{1/2} [K' E(\delta) + (E' - K') F(\delta)] - k^2 K' \sin \delta, \quad (4.2)$$

and

$$km_0 = \sec \delta \{ (1 - k^2 \sin^2 \delta)^{1/2} + k' \}. \quad (4.3)$$

The incomplete elliptic integrals are defined by

$$\left. \begin{aligned} E(\delta) &= \int_0^{\delta} (1 - k^2 \sin^2 u)^{1/2} du \\ F(\delta) &= \int_0^{\delta} (1 - k^2 \sin^2 u)^{-1/2} du, \end{aligned} \right\} \quad (4.4)$$

and the complete elliptic integrals E and K by

$$E = E(\pi/2), \quad K = F(\pi/2). \quad (4.5)$$

Primed letters for complete elliptic integrals indicate that the modulus has been replaced by the co-modulus k' ($k^2 + k'^2 = 1$).

The assumption that k' is small leads to series expansions valid for small values of the cavitation number. Thus, from (4.2),

$$g(\delta) = \frac{1}{4} \pi k'^2 \tan \delta \sec \delta \{1 + O(k'^2)\},$$

and hence equations (4.1) take the form

$$\left. \begin{aligned} \frac{1}{2} km_{0w0} &= \frac{1}{2} (\pi + 4) k'^2 \tan \delta \sec \delta \{1 + O(k'^2)\}, \\ \frac{1}{2} km_{0wx0} &= gd^{-1} \delta \{1 + O(k'^2)\}, \\ \frac{1}{2} km_{0wy0} &= k' \delta \sec \delta \left\{1 + \frac{\pi}{4} k' \frac{\tan \delta}{\delta} + O(k'^2)\right\}, \\ kwc_{D/4m_0} &= \frac{1}{4} \pi k'^2 \tan \delta \sec \delta \{1 + O(k'^2)\}, \end{aligned} \right\} \quad (4.6)$$

and (4.3) becomes

$$km_0 = 1 + k' \sec \delta + O(k'^2). \quad (4.7)$$

On dividing the last three of equations (4.6) by the first, the dimensions of the cavity are expressed in terms of the width of the cavitating plate; thus

$$\left. \begin{aligned} \frac{x_2}{c} &= \frac{4gd^{-1} \delta \sec \delta}{(\pi + 4) k'^2 \tan \delta} \{1 + O(k'^2)\}, \\ \frac{y_2}{c} - \frac{\pi}{\pi + 4} &= \frac{4\delta}{(\pi + 4) k' \tan \delta} \{1 + O(k'^2)\} \\ \text{and } \frac{c_D}{m_0} &= \frac{2\pi}{\pi + 4} \{1 + O(k'^2)\}. \end{aligned} \right\} \quad (4.8)$$

The equations (4.8) involve the two parameters δ , which broadly represents the effect of the tunnel size, and k' , which broadly represents the effect of cavitation number. We shall now separate these two effects, so far as this is possible, by writing \bar{x}_0 , \bar{y}_0 and \bar{C}_D for the limiting forms of x_0 , y_0 and C_D , respectively, as δ tends to zero, that is to say, as the tunnel cross-section increases indefinitely. First making the substitution, obtained from (4.7),

$$k' \sec \delta = \frac{1}{2} Q \left\{ 1 - \frac{1}{2} Q + O(Q^2) \right\}, \quad (4.9)$$

we find that

$$\left. \begin{aligned} \frac{\bar{x}_0}{c} &= \frac{16}{\pi k} \frac{1 + Q + O(Q^2)}{Q^2} \\ \frac{\bar{y}_0}{c} - \frac{\pi}{\pi k} &= \frac{8}{\pi k} \frac{1 + \frac{1}{2} Q + O(Q^2)}{Q} \\ \text{and } \bar{C}_D &= \frac{2\pi}{\pi k} \left\{ 1 + Q + O(Q^2) \right\}, \end{aligned} \right\} \quad (4.10)$$

where the right-hand members are functions of Q only. The corresponding correction factors, expressing the effect of tunnel size, are then found to be

$$\left. \begin{aligned} \frac{x_0}{\bar{x}_0} &= \frac{gd^{-1}\delta}{\sin \delta} \left\{ 1 + O(Q^2) \right\}, \\ \frac{y_0 - \frac{\pi}{\pi k} c}{\bar{y}_0 - \frac{\pi}{\pi k} c} &= \frac{\delta}{\sin \delta} \left\{ 1 + O(Q^2) \right\} \\ \text{and } \frac{C_D}{\bar{C}_D} &= 1 + O(Q^2). \end{aligned} \right\} \quad (4.11)$$

It will be noticed that these correction factors are not entirely independent of the cavitation number, although when the cavitation number is small the inter-dependence is only slight.

The precise physical significance of δ is apparent from (4.6), which shows that it is related to the length of the cavity by the equation

$$\frac{1}{2} \pi x_0 = gd^{-1}\delta \left\{ 1 - \frac{1}{2} Q + O(Q^2) \right\}. \quad (4.12)$$

Accordingly we plot in Fig. 3 the behaviour of \bar{x}_0/x_0 and \bar{y}_0/y_0 as functions of x_0 in the limiting case when $Q = 0$, (Q is then negligible in comparison with y_0 or \bar{y}_0) using δ as a parameter.

Up to this point no restrictions have been imposed on the parameter δ , which is free to range from zero to $\frac{1}{2}\pi$. Accordingly our results are valid, for small values of Q , whatever may be the ratio of the length of the cavity to the width of the tunnel. It should be noticed however, that, as Simmons pointed out, the ratio of the width of the cavity to the width of the tunnel must necessarily be small when Q is small.

We now particularize our results to the case of cavities which are short compared with the width of the tunnel. Then δ is small and the equations (4.11) reduce, by virtue of (4.12), in the case of vanishingly small cavitation number, to

$$\left. \begin{aligned} x_0\sqrt{\bar{x}_0} &= 1 + \frac{\pi^2}{12} x_0^2 + O(x_0^4), \\ y_0\sqrt{\bar{y}_0} &= 1 + \frac{\pi^2}{24} x_0^2 + O(x_0^4) \end{aligned} \right\} (Q = 0) \quad (4.13)$$

and $C_D/\bar{C}_D = 1.$

These results may be simply expressed in words as follows:

(i) For small values of the cavitation number the ratio of the length of a cavity to the width of the stream may be of any order of magnitude, although the width of the bubble is necessarily small compared with either of these dimensions.

(ii) The true drag coefficient of the cavity tends to be independent of the blockage ratio, for small cavitation numbers.

(iii) When the ratio of the length of the cavity to the width of the stream is small, and the cavitation number is also small, the length and breadth of the cavity are both increased by an amount proportional to the square of this ratio, and the proportionate effect on the length is twice as great as that on the breadth.

(b) Free jet

In the case of the free jet, one of the present authors has adapted Simmons's results to a form which furnishes a suitable starting point for the present treatment. Thus, from equations (3.8), (3.9) and (3.10) of ref. 4 we have

$$\left. \begin{aligned}
 \frac{1}{2} \pi m_0 c &= 4 q^{1/2} \sum_{s=0}^{\infty} q^s C_s(\kappa') , \\
 \frac{1}{2} \pi m_0 x_0 &= 4 q^{1/2} \sum_{s=0}^{\infty} q^s X_s(\kappa') , \\
 \frac{1}{2} \pi m_0 y_0 &= 4 q^{1/2} \sum_{s=0}^{\infty} q^s Y_s(\kappa') \\
 \text{and} \quad \frac{1}{2} \pi c D_D / m_0 &= 4 q^{1/2} \sum_{s=0}^{\infty} q^s D_s(\kappa') ,
 \end{aligned} \right\} (4.14)$$

where

$$\kappa' = Q/(2 + Q) \quad (4.15)$$

and $C_s(\kappa')$, $X_s(\kappa')$, $Y_s(\kappa')$, $D_s(\kappa')$ are known functions. In one respect these initial equations are simpler than those (4.1,2,3) for the closed tunnel, since one of the mathematical parameters, namely κ' , depends on the cavitation number Q only. On the other hand, of course, they possess the compensating disadvantage of involving infinite series. The other mathematical parameter, namely q , represents broadly the effect of tunnel size and is accordingly analogous to δ in the previous case.

In order to study the case of small cavitation numbers, we expand each of the coefficients of q^s in equations (4.14) as series in ascending powers of κ' and obtain the following results

$$\left. \begin{aligned}
 \frac{1}{2} \pi m_0 c &= (\pi + 4) q^{1/2} \Gamma_1(q) \kappa'^2 \{1 + O(\kappa'^2)\} , \\
 \frac{1}{2} \pi m_0 x_0 &= 4 q^{1/2} \Gamma_2(q) \{1 + O(\kappa'^2)\} , \\
 \frac{1}{2} \pi m_0 y_0 &= q^{1/2} [4 \Gamma_3(q) \kappa' + \pi \Gamma_1(q) \kappa'^3] \{1 + O(\kappa'^2)\} \\
 \text{and} \quad \frac{1}{2} \pi c D_D / m_0 &= 2 \pi q^{1/2} \Gamma_1(q) \kappa'^2 \{1 + O(\kappa'^2)\} ,
 \end{aligned} \right\} (4.16)$$

where

$$\left. \begin{aligned}
 \Gamma_1(q) &= 1 + 4 q + 6 q^2 + 8 q^3 + O(q^4) , \\
 \Gamma_2(q) &= 1 + \frac{8}{3} q + \frac{8}{3} q^2 + \frac{8}{7} q^3 + O(q^4) \\
 \text{and} \quad \Gamma_3(q) &= 1 + \frac{8}{3} q + \frac{28}{9} q^2 + \frac{48}{7} q^3 + O(q^4) .
 \end{aligned} \right\} (4.17)$$

Division of the latter three equations of (4.16) by the first gives expressions for the cavity dimensions in terms of the width of the cavitating plate, thus

$$\left. \begin{aligned} \frac{x_0}{c} &= \frac{4\Gamma_2(q)}{(\pi+4)\Gamma_1(q)} \frac{1+O(\kappa'^2)}{\kappa'^2}, \\ \frac{y_0}{c} - \frac{\pi}{\pi+4} &= \frac{4\Gamma_2(q)}{(\pi+4)\Gamma_1(q)} \frac{1+O(\kappa'^2)}{\kappa'^2}, \\ \text{and } \frac{C_D}{m_0^2} &= \frac{2\pi}{\pi+4} \{1 + O(\kappa'^2)\}. \end{aligned} \right\} \quad (4.18)$$

The similarity between equations (4.18) for the free jet and (4.8) for the closed tunnel is already clear, and it is perhaps worth mentioning in passing that the relation between k' and κ' is

$$\kappa' = \tanh \left\{ \frac{\pi}{2K(k)} \tanh^{-1} k' \right\}, \quad (4.19)$$

so that κ' and k' tend to equality when small.

Proceeding as in the earlier case, we now write \bar{x}_0 , \bar{y}_0 and \bar{C}_D for the limiting forms of x_0 , y_0 and C_D , respectively, as q tends to zero, that is to say, as the tunnel cross-section increases indefinitely. On using equation (4.15), this leads at once to a restatement of equations (4.10), shewing that our two definitions of \bar{x}_0 , \bar{y}_0 and \bar{C}_D are, in fact, consistent. The corresponding correction factors, expressing the effect of tunnel size, are found to be

$$\left. \begin{aligned} \frac{x_0}{\bar{x}_0} &= \frac{\Gamma_2(q)}{\Gamma_1(q)} \{1 + O(q^2)\}, \\ \frac{y_0 - \frac{\pi}{\pi+4} c}{\bar{y}_0 - \frac{\pi}{\pi+4} c} &= \frac{\Gamma_2(q)}{\Gamma_1(q)} \{1 + O(q^2)\}, \\ \text{and } \frac{C_D}{\bar{C}_D} &= 1 + O(q^2). \end{aligned} \right\} \quad (4.20)$$

* See note at end of this section.

The physical significance of q may be deduced from the second of equations (4.16), which becomes

$$\frac{1}{2} \pi x_0 = 4 q^{1/2} \Gamma_2(q) \left\{ 1 - \frac{1}{2} Q + O(Q^2) \right\}. \quad (4.21)$$

Using q as a parameter, we can now plot in Fig. 3 the variation of x_0/\bar{x}_0 and y_0/\bar{y}_0 as functions of x_0 , in the limiting case when Q vanishes. The above results are true for quite general values of q between 0 and 1, although coefficients of higher powers of q than are contained in (4.17) would be necessary to obtain reasonable accuracy in the evaluation of the functions $\Gamma_1(q)$, $\Gamma_2(q)$ and $\Gamma_3(q)$ when q becomes appreciable in size. The evaluation of further coefficients would be tedious but not difficult.

If, however, we now particularize to the case of small q , that is to say, when the length of the cavity is small compared with the width of the jet, the equations (4.20) reduce, by virtue of (4.21), to the formulae

$$\left. \begin{aligned} x_0 \sqrt{x_0} &= 1 - \frac{\pi^2}{24} x_0^2 + O(x_0^4), \\ y_0 \sqrt{y_0} &= 1 - \frac{\pi^2}{48} x_0^2 + O(x_0^4) \end{aligned} \right\} \quad (Q \rightarrow 0) \quad (4.22)$$

and $C_D \sqrt{C_D} = 1.$

These particular results have already been obtained in an earlier paper, but the general results (4.20, 21) are new.

It will be observed that equations (4.22) are very similar in form to equations (4.13), the only difference being that the coefficients in the case of the free jet are of opposite sign and of half the magnitude of those pertaining to the closed tunnel.

NOTE:

It will be observed that in the limiting case when $Q = 0$, equations (4.11) and (4.20) both imply that the true drag coefficient is completely independent of cavity size. This statement, however, has not a great deal of practical significance since in this limiting case the cavitating head itself must vanish. This is clear from equations (4.6) and (4.16), for c vanishes with k' (or κ'), whatever the value of δ (or q).

At first sight this result, as regards the free jet, seems to be at variance with previous results (see for example, refs. 4 and 6), where the variation of the true drag coefficient at vanishing cavitation number is actually studied quantitatively. There is in fact, however, no contradiction, since in the earlier papers the cavity was allowed to be open at the rear, whilst in the present paper it is necessarily closed.

5. First-order theory for axially symmetric cavities

With the results of the exact two-dimensional theory to act as a guide, we are now in a position to develop the first order formulae from the approximate axially symmetric theory.

Since it is required to compare the properties of cavities in bounded and unbounded streams at a given value of the cavitation number, the fundamental connection is

$$m_0 = \bar{m}_0 . \quad (5.1)$$

For the other variables, we express the bounded stream value as the sum of the unbounded stream value and a small increment. Thus, for example, the equation (3.13) evaluated at the equator of the cavity becomes

$$(m_0 - 1)(\bar{U} + \Delta U) = \bar{\mu}_0 + \Delta\mu_0 - \tanh \bar{\mu}_0 - \operatorname{sech}^2 \bar{\mu}_0 \Delta\mu_0 + \frac{2}{3} C_{\nu,2} f^3 + R \quad (5.2)$$

where R will be used to denote a remainder composed of smaller order terms. On the other hand, equation (2.6) evaluated at the equator of the cavity becomes

$$(\bar{m}_0 - 1) \bar{U} = \bar{\mu}_0 - \tanh \bar{\mu}_0 , \quad (5.3)$$

and accordingly, by subtraction,

$$(m_0 - 1) \Delta U = \tanh^2 \bar{\mu}_0 \Delta\mu_0 + \frac{2}{3} C_{\nu,2} f^3 + R . \quad (5.4)$$

Similarly, since the value of μ at the point $(0, y_0)$ is μ_0 , we find from equations (3.5, 6 and 7) that

$$\bar{U} + \Delta U = \frac{1}{2} \sinh 2 \bar{\mu}_0 + \cosh 2 \bar{\mu}_0 \Delta\mu_0 - \bar{\mu}_0 - \Delta\mu_0 - \frac{2}{3} C_{\nu,2} f^3 + R , \quad (5.5)$$

whilst, from (2.3),

$$\bar{U} = \frac{1}{2} \sinh 2 \bar{\mu}_0 - \bar{\mu}_0 . \quad (5.6)$$

A subtraction now yields the result

$$\Delta U = 2 \sinh^2 \bar{\mu}_0 \Delta\mu_0 - \frac{2}{3} C_{\nu,2} f^3 + R . \quad (5.7)$$

Again, the value of μ at the point $(x_0, 0)$ is μ_∞ , i.e. $\bar{\mu}_\infty + \Delta\mu_\infty$, so that (3.5, 6 and 7), together with (2.3, 4) give a result precisely similar to (5.7), but with the subscript ∞ replacing the subscript 0 throughout. Since, however, we have already noticed (2.4) that $\bar{\mu}_0 = \bar{\mu}_\infty$ it follows that $\mu_0 = \mu_\infty$, and the cavity in the bounded stream is still a prolate spheroid, to the present order of accuracy. This fact is also clear directly from (3.6).

Elimination of \bar{U} between equation (5.3) and (5.6) yields an expression for $(\bar{m}_0 - 1)$, which may be equated to a similar expression obtained by eliminating ΔU from (5.4) and (5.7), thus

$$\frac{\bar{\mu}_0 - \tanh \bar{\mu}_0}{\frac{1}{2} \sinh 2 \bar{\mu}_0 - \bar{\mu}_0} = \frac{\tanh^2 \bar{\mu}_0 \Delta\mu_0 + \frac{2}{3} C_{V,2} f^3 + R}{2 \sinh^2 \bar{\mu}_0 \Delta\mu_0 - \frac{2}{3} C_{V,2} f^3 + R} \quad (5.8)$$

Now, when the cavitation number is very small, these two expressions for $(\bar{m}_0 - 1)$ must tend to zero and hence $\bar{\mu}_0$ must tend to infinity. Both the numerator and the denominator of the left-hand member of (5.8) are then clearly dominated by the leading terms. It may then be deduced that, in the right-hand member of (5.8), the numerator is dominated by the second term, whilst the denominator is dominated by the first term. It follows, since $\sinh 2 \bar{\mu}_0 \sim 2 \sinh^2 \bar{\mu}_0$, that

$$2 \bar{\mu}_0 \Delta\mu_0 \sim \frac{2}{3} C_{V,2} f^3 \quad (\bar{\mu}_0 \rightarrow \infty). \quad (5.9)$$

In order to deduce the corresponding change in the proportions of the cavity, observe that, from (1.3),

$$y_0/x_0 = \operatorname{sech} \mu_0,$$

so that

$$\frac{\Delta(y_0/x_0)}{y_0/x_0} = - \tanh \bar{\mu}_0 \Delta\mu_0. \quad (5.10)$$

Combining (5.9) and (5.10), we find that

$$\frac{\Delta(y_0/x_0)}{y_0/x_0} \sim - \frac{C_{V,2} f^3}{3 \bar{\mu}_0} \quad (\mu_0 \rightarrow \infty). \quad (5.11)$$

The numerical values of $-C_{V,2}$ are given in Appendix II as

$$-C_{0,2} = .205911\dots \quad -C_{1,2} = -.796821\dots, \quad (5.12)$$

so that the corrections to be applied in a closed tunnel are of opposite sign, and roughly four times in magnitude, those to be applied in a free jet. This makes a reasonable comparison with the two-dimensional case, where the corresponding factor is exactly two.

Again, the corrections to be applied are proportional to the cube of the ratio of the length of the cavity to the width of the axially symmetric jet, whilst in two dimensions the corrections were proportional to the square of this ratio.

There is an important dissimilarity between the two-dimensional and axially symmetric results, however, in that the numerical coefficient in the latter case tends logarithmically to zero with the cavitation number, whereas in the two-dimensional case it tends to a finite limit.

6. Use of the drag coefficients to determine cavity dimensions

The width of the cavitating plate, namely $2c$, does not appear in the analysis which we have developed for the axially symmetric cavity, so that it is impossible to determine unaided the variation of the actual cavity dimensions, as distinct from the thickness ratio y_0/x_0 . However, it is clear from the two-dimensional theory that the true drag coefficient C_D , based on the cavitating plate width, is very insensitive to boundary effects, and by assuming that the same is true in the axially symmetric case we can calculate the variation of x_0 and y_0 separately.

From equations (1.7, 8), the true drag coefficient is given by

$$C_D = (y_0^2/c^2) C'_D, \quad (6.1)$$

where
$$C'_D = Q - \sinh^2 \mu_0 I(\mu_0), \quad (6.2)$$

and
$$I(\mu_0) = 2 f^{-2} \int_{y_0}^1 (m-1)^2 y \, dy. \quad (6.3)$$

Taking logarithms in equation (6.1) and subsequently performing the operation Δ , we find that, since $C_D = \bar{C}_D$ by assumption,

$$2 \frac{\Delta y_0}{y_0} = - \frac{\Delta C'_D}{C'_D}. \quad (6.4)$$

The cavitation number Q is the same in both bounded and unbounded cases, so that

$$- \Delta C'_D = \sinh^2 \bar{\mu}_0 \Delta \mu_0 I(\bar{\mu}_0) + \sinh^2 \bar{\mu}_0 \Delta I(\mu_0). \quad (6.5)$$

On making the transformation to the conicoidal coordinates (1.1) and remembering that the path of integration is along $\lambda = 0$, (6.3) becomes

$$I(\mu_0) = 2 \int_{\sinh^{-1} f}^{\mu_0} (m-1)^2 \operatorname{cosech}^2 \mu \coth \mu \, d\mu, \quad (6.6)$$

whence, in particular,

$$\bar{U}^2 I(\bar{\mu}_0) = 2 \bar{\mu}_0 \coth \bar{\mu}_0 - 2 \ln \cosh \bar{\mu}_0 - \bar{\mu}_0^2 \operatorname{cosech}^2 \bar{\mu}_0 - 1, \quad (6.7)$$

and

$$I(\bar{\mu}_0) \sim (\ln 4 - 1)/\bar{U}^2 \quad (\mu_0 \rightarrow \infty). \quad (6.7a)$$

The quantity $\Delta I(\mu_0)$ may be evaluated from (6.6) as the sum of four parts, thus

$$\Delta I(\mu_0) = \Delta_1 + \Delta_2 + \Delta_3 + \Delta_4, \quad (6.8)$$

where $\Delta_1 = 2 (\bar{m}_0 - 1)^2 \operatorname{cosech}^2 \bar{\mu}_0 \coth \bar{\mu}_0 \Delta \mu_0 + R$

$$\sim \frac{2}{3} C_{\nu,2} f^3 (\bar{m}_0 - 1) \quad (\mu_0 \rightarrow \infty); \quad (6.9)$$

and $\Delta_2 = -2 \int_0^{\sinh^{-1} f} (\bar{m} - 1)^2 \operatorname{cosech}^2 \mu \coth \mu \, d\mu + R$

$$\sim \frac{f^4}{18\bar{U}^2} \quad (\mu_0 \rightarrow \infty). \quad (6.10)$$

The two contributions Δ_1 and Δ_2 result from the alteration of the upper and lower limits of integration in $I(\mu_0)$. The remaining contributions, Δ_3 and Δ_4 , result from applying the operator Δ to the integrand. For a given value of μ , the only factor in the integrand which is susceptible to Δ is $(m-1)^2$. Now, from (3.13) and (2.6)

$$\Delta\{(m-1) U\} = \bar{U} \Delta(m-1) + (\bar{m}-1) \Delta U = \frac{2}{3} C_{\nu,2} f^3 + R$$

so that $\bar{U} \Delta(m-1) \sim \frac{2}{3} C_{\nu,2} f^3 - (\bar{m}-1) \Delta U$. (6.11)

On using this result we now find that

$$\Delta_3 = 4 \times \frac{2}{3} C_{v,2} \frac{f^3}{\bar{U}} \int_0^{\bar{\mu}_0} (\bar{m}-1) \operatorname{cosech}^2 \mu \coth \mu d\mu + R$$

$$\sim \frac{\frac{4}{3} C_{v,2} f^3}{\bar{U}^2} \quad (\mu_0 \rightarrow \infty); \quad (6.12)$$

and

$$\Delta_4 = \frac{2\Delta U}{\bar{U}} I(\bar{\mu}_0) + R$$

$$\sim -\frac{4}{3} C_{v,2} f^3 \frac{(\ln 4 - 1)}{\bar{\mu}_0 \bar{U}^2} \quad (\mu_0 \rightarrow \infty). \quad (6.13)$$

It is clear that when f is small, and when $\mu_0 \rightarrow \infty$ that is to say, when the cavitation number is also small, Δ_1 , Δ_2 and Δ_4 are all small compared with Δ_3 , so that equation (6.5) becomes

$$-\Delta C'_D \sim \left[\frac{\sinh 2\bar{\mu}_0}{2\bar{\mu}_0} \frac{(\ln 4 - 1)}{\bar{U}^2} + \frac{2\sinh^2 \bar{\mu}_0}{\bar{U}^2} \right] \frac{2}{3} C_{v,2} f^3. \quad (6.14)$$

The first term inside the square bracket may be neglected by comparison with the second term, when $\bar{\mu}_0$ is large.

Examining the relative magnitude of the terms in (6.2), we find from (5.8) that

$$Q \sim 2(\bar{m}_0 - 1) \sim 2 \bar{\mu}_0 / \sinh^2 \bar{\mu}_0 \quad (\mu_0 \rightarrow \infty), \quad (6.15)$$

and from (2.3) and (6.7a) that

$$\sinh^2 \bar{\mu}_0 I(\bar{\mu}_0) \sim (\ln 4 - 1) \cosh^2 \bar{\mu}_0 \quad (\mu_0 \rightarrow \infty); \quad (6.16)$$

so that the second item is negligible compared with the first.

Substitution of the results (6.14, 15 and 16) in equation (6.4) produces the result

$$\frac{\Delta y_0}{\bar{y}_0} \sim \frac{\frac{2}{3} C_{v,2} f^3 \sinh^2 \bar{\mu}_0}{\cosh^2 \bar{\mu}_0 \cdot 2 \bar{\mu}_0}$$

$$\sim \frac{C_{v,2} f^3}{3 \bar{\mu}_0} \quad (\mu_0 \rightarrow \infty). \quad (6.17)$$

Finally, since

$$\ln x_0 = \ln y_0 - \ln (y_0/x_0) ,$$

we find, on applying the operator Δ , that

$$\frac{\Delta x_0}{x_0} = \frac{\Delta y_0}{y_0} - \frac{\Delta(y_0/x_0)}{y_0/x_0}$$

$$\sim \frac{2Cv_2 f^3}{3 \mu_0} \quad (\mu_0 \rightarrow \infty), \quad (6.18)$$

by virtue of (5.11) and (6.17).

The results (6.17) and (6.18) for the axially symmetric cavity are analogous with those (4.13 and 22) for the two-dimensional cavity. They state, in fact, that, for a small axially symmetric cavity at low cavitation number in a closed or open tunnel of circular cross section, the boundary effect is proportional to the cube of the ratio of cavity length to tunnel breadth, and the proportionate effect on the cavity length is twice as great as that on the cavity breadth. Furthermore, the boundary effect is a shrinkage in the case of the open jet and an expansion in the case of the closed tunnel, the latter effect being roughly four times as great as the former.

7. Numerical results

The simple first order results deduced in sections 5 and 6 apply only to the doubly limiting case when both Q and f (or x_0) are very small. One of these limitations, that of small cavitation number, applies also to the more general theory developed in sections 2 and 3, for the prolate spheroids investigated therein satisfy the constant pressure condition of cavitating flow only when the thickness ratio y_0/x_0 is very small.

The condition that the length of the cavity should be small compared with the width of the tunnel, however, is not necessary to ensure the validity of the theory of sections 2 and 3. It is true that the width of the cavity must be small, in order that the mathematical boundary condition applied to the surface of the free jet shall satisfactorily represent the actual physical boundary condition. But for any given cavity length, the width of the cavity is bound to be small when the cavitation number is small enough, so that we do not need to stipulate that, in addition, the length of the cavity shall be small.

Accordingly, it seems worth while to evaluate the results of the general theory for a wide range of values of the non-dimensional cavity length x_0 , and for various small values of Q . In order to be convenient for practical use, the results have to present, for given values of Q , the variation of the thickness ratio y_0/x_0 as a function of some easily measured length, such as x_0 . In view of the fact that Q is only obtained in terms of x_0 , y_0 and f after a fairly lengthy calculation, some care is necessary in order to reduce to a minimum the labour and inaccuracy involved by inverse interpolation. The method of calculation which was eventually selected will be briefly described.

The cavity in a bounded stream, at a given value of the cavitation number Q , is characterized by a trio of values μ_0 , y_0 and f , connected by the relation (1.3). This value of μ_0 corresponds, in an unbounded stream, to a slightly different value of the cavitation number, which we shall denote by $\bar{Q}_y = G(\mu_0)$.

Similarly, the cavity in the bounded stream is characterized, for given Q , by the trio μ_{∞} , x_0 and f , connected by the relation (1.3). We accordingly define $\bar{Q}_x = G(\mu_{\infty})$, that is to say, the cavitation number in the unbounded stream which would yield a cavity of the length actually observed in the bounded stream.

The essence of our method is to form estimates of \bar{Q}_y and \bar{Q}_x from the given value of Q and hence by using (2.7) to calculate μ_0 and μ_{∞} , which yield the required values of y_0 and x_0 . The process is iterative, since each estimate of y_0 and x_0 enables a better estimation of \bar{Q}_y and \bar{Q}_x to be made, and these in turn lead to improved estimates of y_0 and x_0 .

The first step was to tabulate \bar{Q} as a function of $\bar{\mu}_0$, using (2.7), at intervals sufficiently close to make inverse interpolation simple and accurate (Table I). Next, taking in turn the values $y = 0.05$ (0.05) 0.35, combined with the values $f = 0.5$ (0.5) 2.0, the function $U(y_0, f)$ was calculated from (3.5) by setting $\Omega(0, y_0) = 0$. For the same values of y_0 and f , the product $(m_0 - 1)U$ was also calculated from equation (3.13). Simple division then yielded m_0 , from which \bar{Q} followed by virtue of (1.6). For the same ratios y_0/f , the function \bar{Q}_y was calculated directly from (2.7). With f as a parameter, the difference $\bar{Q}_y - Q$ was tabulated as a function of y_0 , and the resulting second differences were sufficiently steady to ensure satisfactory direct interpolation (Table II).

In a similar manner, but setting $\Omega(x_0, 0) = 0$ in place of $\Omega(0, y_0) = 0$, the function $\bar{Q}_x - Q$ was tabulated as a function of x_0 , with f as a parameter, intervals of 0.02 in the argument being quite small enough to ensure accurate interpolation (Table III).

For a given value of Q and one of the tabular values of f , the first estimate of \bar{Q}_y (or \bar{Q}_x) was simply Q itself. The corresponding value of μ_0 (or μ_{∞}), obtained by inverse interpolation from Table I, yielded a first estimate of y_0 (or x_0). The corresponding estimate of the difference $\bar{Q}_y - Q$ (or $\bar{Q}_x - Q$) was interpolated from Table II (or III) and an improved estimate of \bar{Q}_y (or \bar{Q}_x) thus obtained. The cycle was repeated until the value of y_0 (or x_0) so obtained was not subject to further change, when it was assumed to be correct. Convergence of the process was rapid.

The advantage of this method of computation is that the use of the unwieldy formulae involving infinite series, which are applicable to bounded streams, is kept to an absolute minimum. The only inverse interpolation required is for the comparatively simple relation (2.7), which applies to an unbounded stream.

The calculations of C_D were planned on similar principles, this being rendered even more important owing to the fact that numerical integration was involved. The expression (1.8) for C_D was split into parts, thus

$$C_D' = Q - (A - B)/U^2, \quad (7.1)$$

$$\left. \begin{aligned} \text{where } A &= 2 y_0^2 \int_{u_0}^1 (\bar{m} - 1)^2 \bar{U}^2 y \, dy \\ \text{and } B &= 2 y_0^2 \int_{u_0}^1 \{(\bar{m} - 1)^2 \bar{U}^2 - (m - 1)^2 U^2\} y \, dy. \end{aligned} \right\} (7.2)$$

The small numerical integral B was tabulated (Table V) for the same values of y_0 and f as those used in the compilation of Table II. Then for one of the chosen values of Q , and a tabular value of f , the previously computed value of y_0 enabled the value of B to be interpolated, whilst the value of A was readily calculated analytically.

The results of our computations are displayed in Figs. 4 - 6. Fig. 4 shows the behaviour of the ratio $(y_0/\bar{x}_0)/(y_0/x_0)$ as a function of x_0 , in the case of the open tunnel of circular cross-section. A corresponding curve for the two-dimensional case is shown dotted for comparison. Fig. 5 shows the same function plotted against the blockage ratio, that is to say, y_0 in the case of the two-dimensional curve, and y_0^2 in the axially symmetric case. Fig. 6 shows the effect of the free stream boundary on the modified drag coefficient based on the cavity diameter. As explained in Section 6, we may draw the inference that the maximum cross-sectional area of the cavity behaves in an approximately reciprocal manner.

NOTE:

When this report was in course of preparation, it was learnt that a closely similar investigation was being conducted at another Government establishment, namely, the Admiralty Research Laboratory, Teddington. It was therefore agreed to divide the field for numerical work between the two establishments. Accordingly, the numerical results depicted in the graphs at the end of this report refer only to open jet tunnels, which are of more particular interest to this establishment. It is understood that a report containing similar results for closed tunnels is being published by A.R.L.

8. Conclusions

The wall corrections necessary to measurements of axially symmetric cavities in circular tunnels of free jet type have been displayed graphically. These results are applicable to small values of the cavitation number but to arbitrary values of the ratio (length of cavity)/(width of cross-section of tunnel) $= x_0$.

For the case when x_0 is small as well as the cavitation number, we have demonstrated the following results:

(a) In two-dimensional flow

(i) the fractional increases (closed tunnel) or decreases (free jet) in the length and width of the cavity are both proportional to x_0^2 . The factors of proportionality are

| | length | width |
|---------------|-------------|-------------|
| closed tunnel | $\pi^2/12$ | $\pi^2/24$ |
| free jet | $-\pi^2/24$ | $-\pi^2/48$ |

(ii) the true drag coefficient, based on the cross-sectional area of the cavitating head, is unaffected by the tunnel boundary.

(b) In axisymmetric flow

(i) the fractional decrease (closed tunnel) or increase (free jet) in the thickness ratio of the cavity is proportional to x_0^3 . The factors of proportionality tend to zero with the cavitation number, but they are in the following ratio:

| | |
|---------------|-----------|
| closed tunnel | - .796824 |
| free jet | + .205911 |

(ii) assuming that the true drag coefficient is unaffected by the boundary, then the fractional increases (closed tunnel) or decreases (free jet) in the length and width of the cavity are both proportional to x_0^3 . The factors of proportionality tend to zero with the cavitation number, but they are in the ratio:

| | length | width |
|---------------|----------------------|------------|
| closed tunnel | $2 \times .796824$ | $.796824$ |
| free jet | $- 2 \times .205911$ | $-.205911$ |

References

1. N. Simmons "The geometry of liquid cavities with especial reference to the effects of finite extent of the stream", A.D.E., Ministry of Supply, Report No. 17/48, Aug. 1948.
2. C.N.H. Lock "The interference of a wind tunnel on a symmetrical body", R. and M. No. 1275, Oct. 1929.
3. H. Lamb "On the effect of the walls of an experimental tank on the resistance of a model", R. and M. No. 1010, Jan. 1926.
4. A.H. Armstrong "Boundary corrections to cavity dimensions and drag coefficient of a two-dimensional plate in a free jet", A.R.E., Ministry of Supply, Report No. 12/51 Oct. 1951.
5. A.H. Armstrong "The transformation of certain series of Bessel functions into series of Legendre polynomials", A.R.E., Ministry of Supply, Report No. 20/51, Dec. 1951.
6. G. Birkhoff, "Wall effects in cavity flow - I", Quart. App. Math. VIII, No. 2., July, 1950.
H. Plesset
and N. Simmons "Wall effects in cavity flow - II", Quart. App. Math. IX, No. 4., Jan. 1952.

Acknowledgement

The authors wish to acknowledge the helpful criticisms received from Dr. N. Simmons of the Armament Design Establishment, while this report was in draft form. In particular, Appendix I was added as a result of these comments.

Appendix I

The validity of the approximate boundary condition at the free surface

The physical boundary condition at the free surface of the jet differs from the approximate mathematical boundary condition in two respects. We have, in fact, satisfied the wrong boundary condition at the wrong place, and it is necessary to see whether the inaccuracies involved are serious.

Owing to the excessive amount of numerical work which would be involved in an exact investigation, we shall restrict ourselves to a numerical check in the plane of symmetry, together with a survey of the order of magnitude only elsewhere.

One of the inaccuracies involved is due to the displacement of the free boundary, and this is obviously a maximum at the plane of symmetry, where we shall assume that the radius of cross-section is $1 + \epsilon$.

The other inaccuracy is due to assuming that the velocity magnitude at the boundary is adequately represented by the axial component of the velocity. This particular error, which vanishes at the plane of symmetry, is obviously a "cosine effect" of the angle of inclination which the free surface makes with the axis. The order of magnitude of the maximum angle involved may be taken as given by ϵ / f .

The equation of the "free boundary" of the jet, when calculated by the present approximate method, is

$$y^2 \left\{ \frac{1}{2} U + \Omega_g(x,y) \right\} = \frac{1}{2} U ,$$

so that

$$\epsilon U = - \Omega_g(0,1) \{ 1 + O(\epsilon) \} . \quad (I.1)$$

Neglecting the factor $\{ 1 + O(\epsilon) \}$ in the right-hand member of (I.1) we have calculated the displacement ϵ as a function of cavitation number and cavity length, the results being shown in Fig. 7.

A more exact theory than the one used in this report would have to apply the free boundary condition at the free surface itself, that is to say, on a surface lying between $y = 1$ and $y = 1 + \epsilon$. It may be seen intuitively that the results of such an improved theory for a given value of f , would lie somewhere between our present results for that value of f and the corresponding results when f is replaced by $f/\sqrt{1 + \epsilon}$. In other words, the plotted points in the Figs. 4 - 6 are a little to the left of their correct position. The horizontal coordinates should be increased by a factor which lies between 1 and $(1 + \epsilon)$, $[(1 + 2\epsilon)$ in the case of Fig. 5]. The small values assumed by ϵ in Fig. 7 make it clear that the correction involved would be small.

The boundary condition which has actually been applied in this report ensures that the axial component of velocity shall be constant on the cylinder $y = 1$. Owing to the displacement of the jet boundary, however, it is clear that this axial component of velocity will not be constant on the jet boundary. Accordingly we shall investigate the difference between the velocity at infinity and the axial component of velocity on the equator of the jet boundary. Ideally, of course, this difference should be zero, since the axial component is at this point equal numerically to the velocity magnitude.

From equation (3.10) the actual difference is given by

$$(1 - m) U = \epsilon \frac{\partial \phi_B}{\partial y} (0, 1) \{1 + O(\epsilon)\} . \quad (I.2)$$

Now, from the definitions (3.2) and (3.9), it can be shown that

$$\frac{\partial \phi}{\partial y} (x, y, \nu, p) = y \Omega(x, y, \nu, p+1) ,$$

from which it follows that, putting $\nu = 0$ for the free boundary,

$$\frac{1}{2} \frac{\partial \phi_B}{\partial y} (0, 1) = -f \Omega(f, 1, 0, 0) + \Omega(f, 1, 0, -1) - \Omega(0, 1, 0, -1) . \quad (I.3)$$

Substituting this formula in (I.2) and using the previously calculated values of ϵ , we can now plot $(1 - m)U$ as a function of Q and x_0 , the results being shown in Fig. 8.

In order to provide a basis of comparison we also show in Fig. 8, by a dashed line, the additional contribution to the axial component of velocity at the centre of the jet due to the presence of the free surface. According to equations (2.6) and (3.13) this may be expressed, after some manipulation, as

$$\left[(\bar{m} - 1) \bar{U} - (m - 1) U \right]_{(x, y) = (0, 0)} = \ln 2 f - 1 - 2f \phi(f, 0, 0, -1) + 2 \phi(f, 0, 0, -2) \quad (I.4)$$

It is clear from Fig. 8 that the variation of the axial component of velocity on the free boundary is of a smaller order than the variations produced at the jet centre by the presence of the free boundary. In fact, the two effects differ by a factor of at least 5 in all the cases used in constructing the curves for Figs. 4 - 6. The centre of the jet is chosen as the point of the basis of comparison because the effect of the free boundary is least there, so that the difference in order of the two effects would be even more marked elsewhere.

Finally, it is necessary to examine the effect of the angle of inclination between the jet boundary and the axis of symmetry. This results, of course, in a discrepancy between the axial component and the magnitude of the velocity. Since this is a cosine effect the order of magnitude is given by the square of the order of magnitude of the angle of inclination, namely $(\epsilon/f)^2$. This is compared with the quantity $(1 - m)$, measuring the variations in axial component, in fig. 9. Clearly the two effects are of the same order, and, since the latter effect has been shown to be unimportant, so is the former.

UNCLASSIFIED

APPENDIX II

It has been shown (ref. 5) by one of the present authors that infinite series of the types appearing in equations (3.2) and (3.9) may be transformed into other series which converge rapidly near the origin. The particular results required in the computation of equations (3.3), (3.4) and (3.11) are listed below.

$$\phi(x,y,\nu,-1) = -\frac{1}{2r} + \sum_{n=0}^{\infty} C_{\nu,n} \frac{r^n P_n(s)}{n!}$$

$$\phi(x,y,\nu,-2) = -\frac{1}{2} \ln \{r(1+s)\} + \sum_{n=0}^{\infty} C_{\nu,n-1} \frac{r^n P_n(s)}{n!}$$

$$\Omega(x,y,\nu,-2) = \frac{1}{2} \{r(1+s)\}^{-1} - \sum_{n=0}^{\infty} C_{\nu,n-1} \frac{r^{n-1} P_n(s)}{(n+1)!}$$

$$\Omega(x,y,\nu,-3) = \frac{1}{2} [\ln \{r(1+s)\} - \frac{1}{2} (1-s)/(1+s)] - \sum_{n=0}^{\infty} C_{\nu,n-2} \frac{r^{n-1} P_n(s)}{(n+1)!}$$

where $r^2 = x^2 + y^2$, $s = x/r$

and $P_n(s)$ is the Legendre polynomial of order n .

The coefficients $C_{\nu,n}$ have the following numerical values:

| | | | |
|------------|-------------|------------|--------------|
| $C_{0,-1}$ | = 0 | $C_{1,-1}$ | = - .375000 |
| $C_{0,0}$ | = + .435345 | $C_{1,0}$ | = + 1.106824 |
| $C_{0,1}$ | = 0 | $C_{1,1}$ | = - 1 |
| $C_{0,2}$ | = - .205911 | $C_{1,2}$ | = .796824 |
| $C_{0,4}$ | = + .658857 | $C_{1,4}$ | = - 1.200470 |
| $C_{0,6}$ | = - 5.14657 | $C_{1,6}$ | = + 7.45829 |
| $C_{0,8}$ | = + 73.7500 | $C_{1,8}$ | = - 96.2205 |
| $C_{0,10}$ | = - 1682.77 | $C_{1,10}$ | = + 2070.91 |

$$C_{\nu,2n+1} = 0 \quad (n > 0).$$

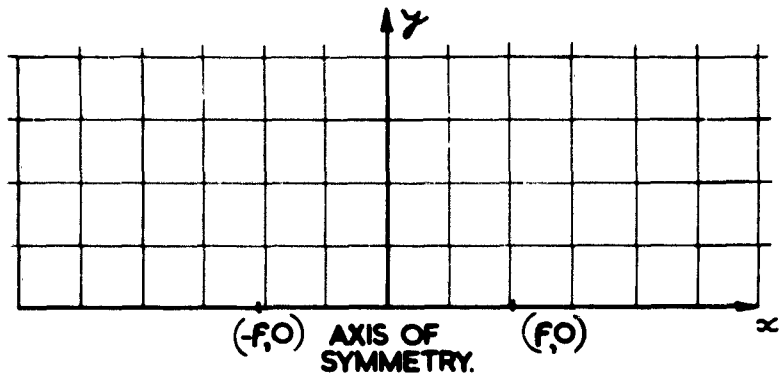


FIG. 1. CYLINDRICAL CO-ORDINATES.

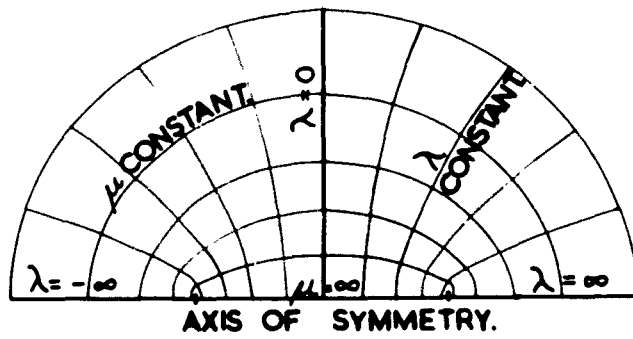


FIG. 2. CONICOIDAL CO-ORDINATES.

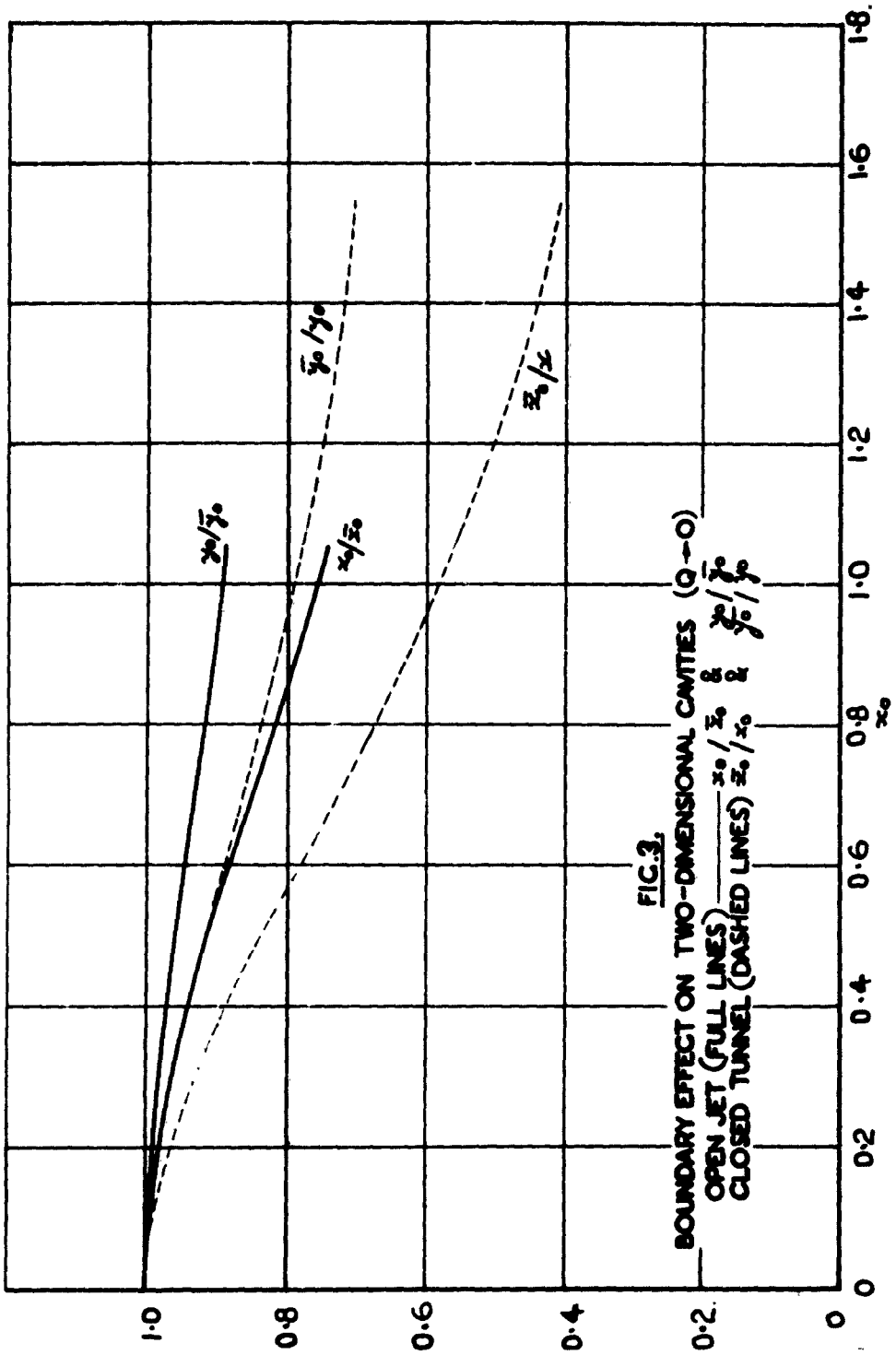
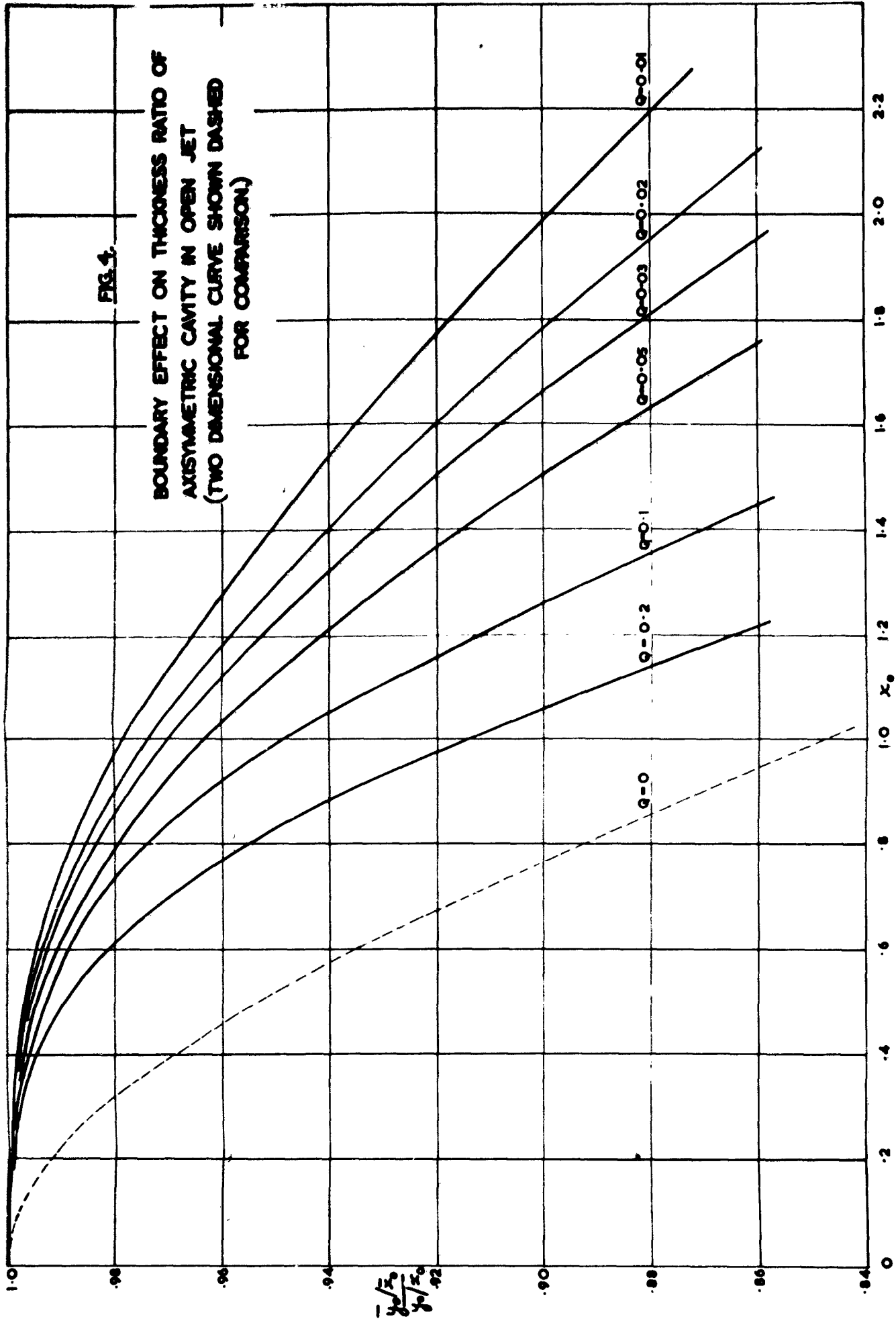


FIG. 3.
 BOUNDARY EFFECT ON TWO-DIMENSIONAL CAVITIES (Q=0)
 OPEN JET (FULL LINES) x_0/\bar{x}_0 & \bar{x}_0/\bar{x}_0
 CLOSED TUNNEL (DASHED LINES) x_0/\bar{x}_0 & \bar{x}_0/\bar{x}_0



7

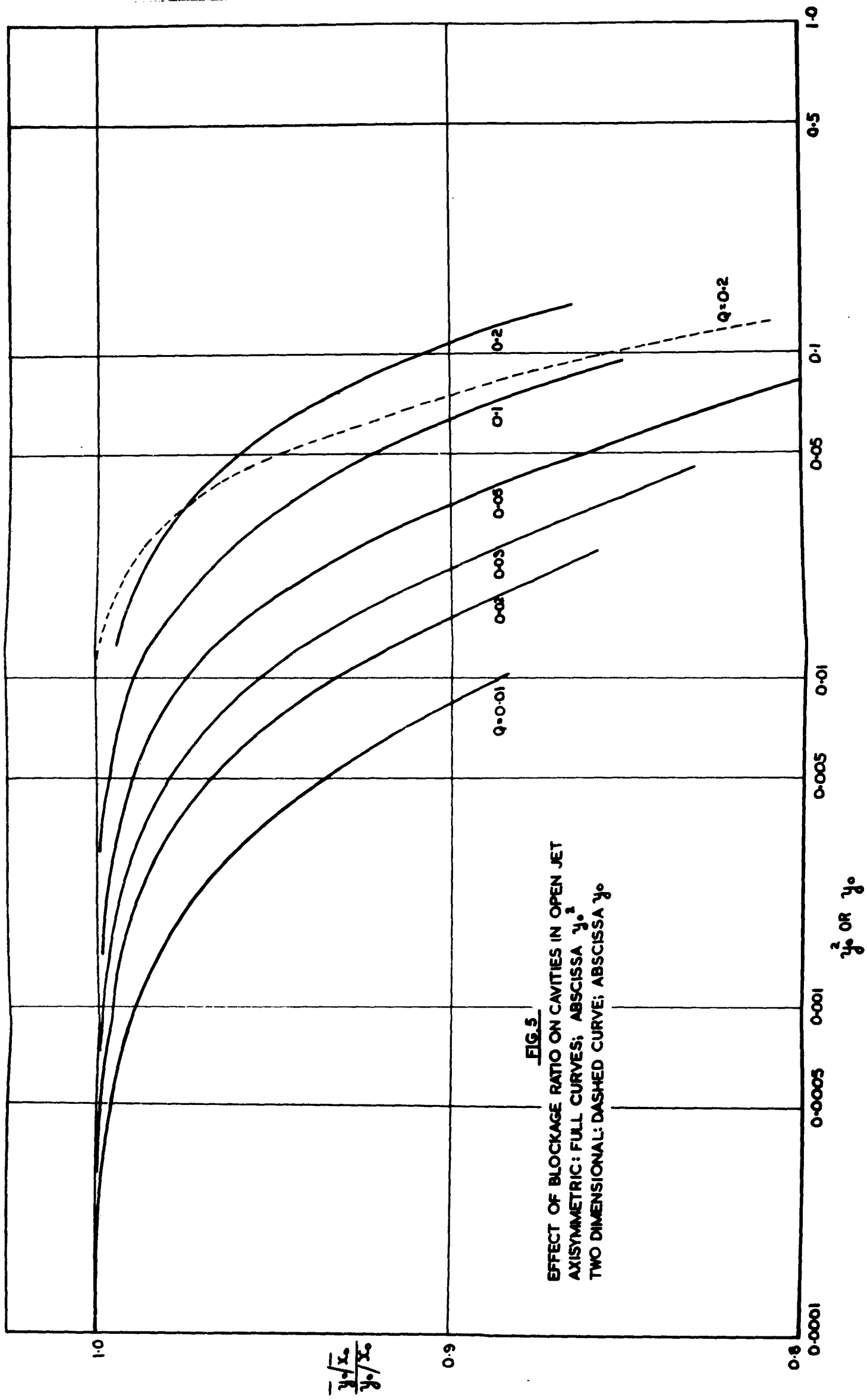


FIG. 5
 EFFECT OF BLOCKAGE RATIO ON CAVITIES IN OPEN JET
 AXISYMMETRIC: FULL CURVES; ABSCISSA y_0^2
 TWO DIMENSIONAL: DASHED CURVE; ABSCISSA y_0

15

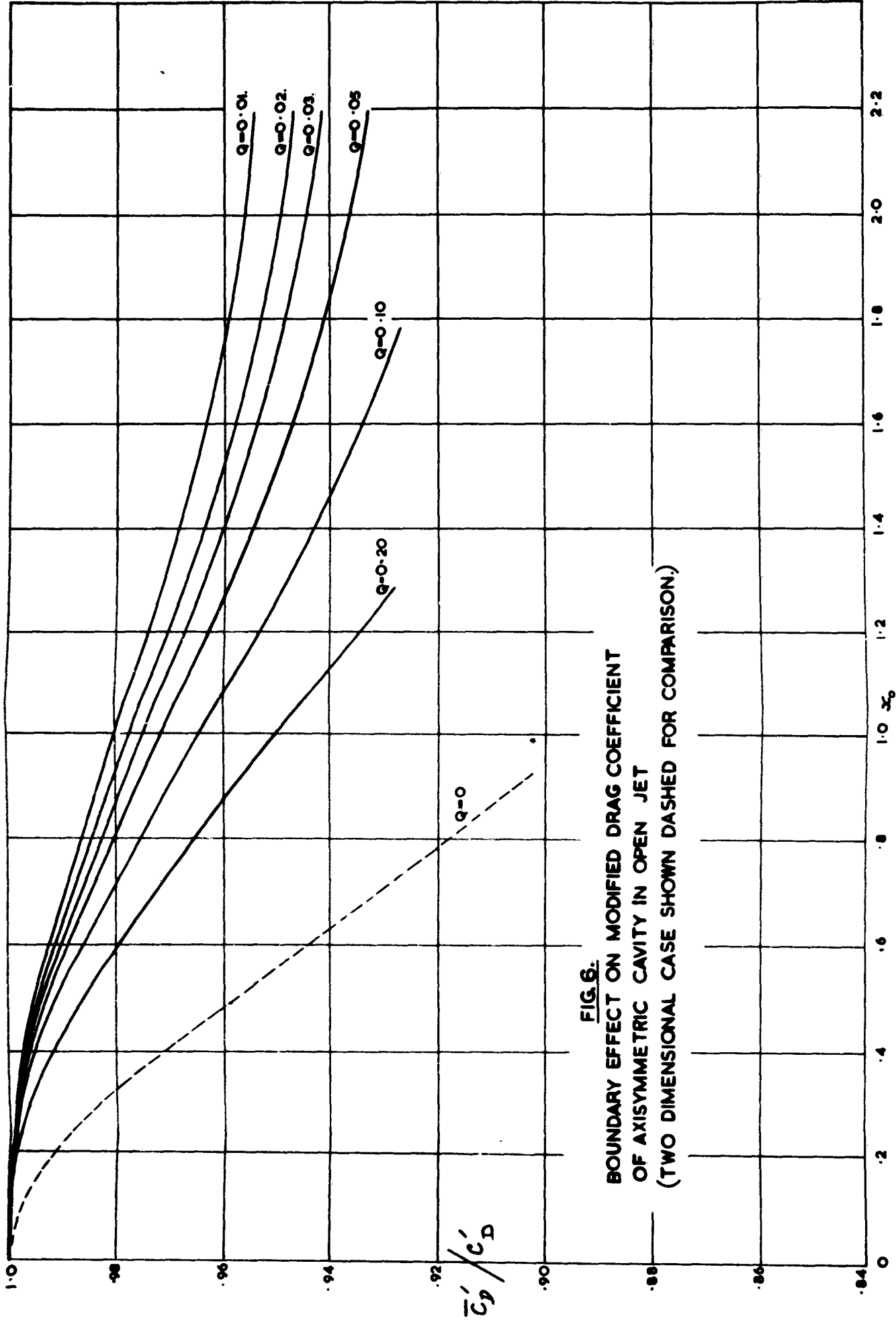
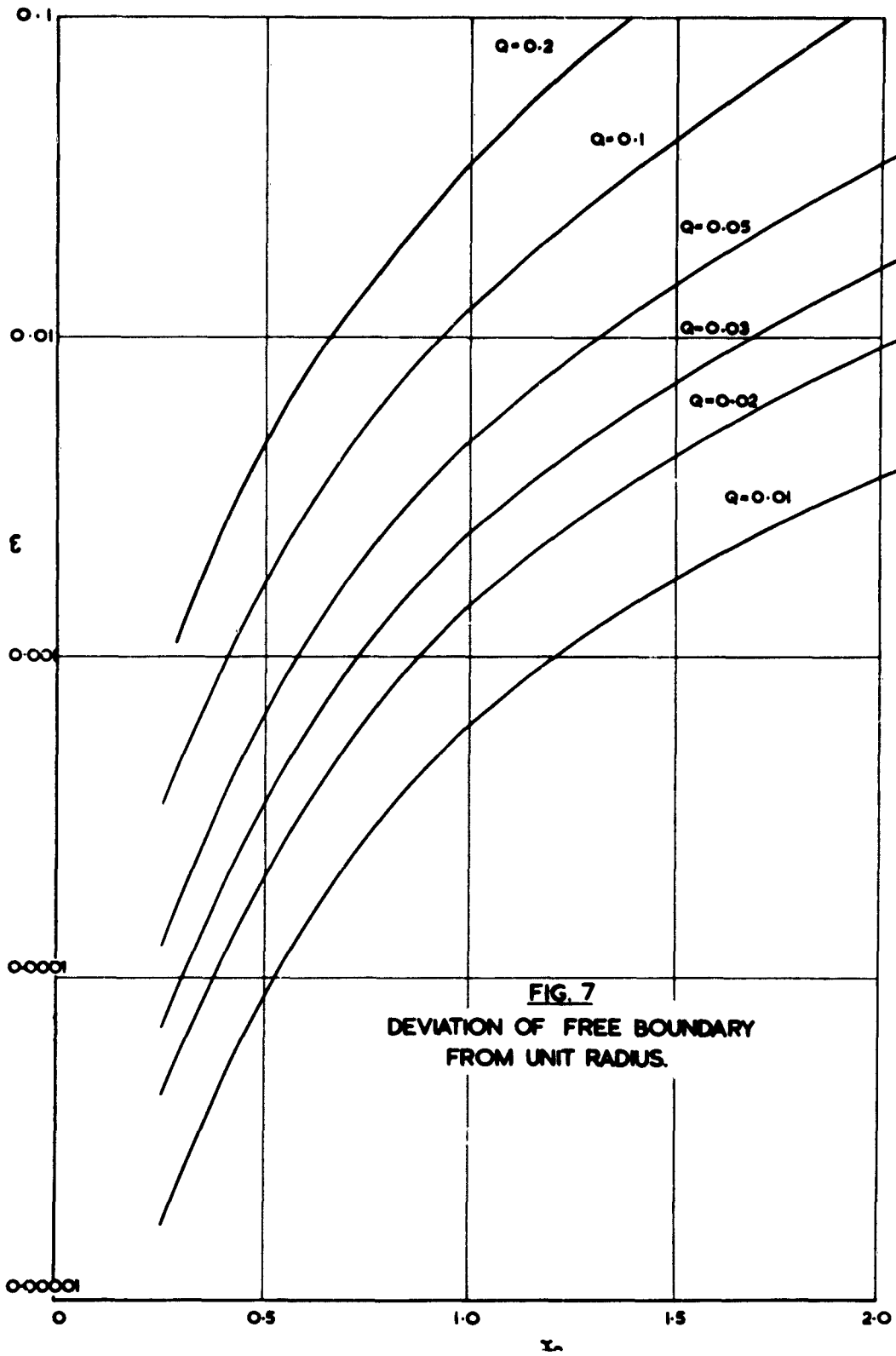
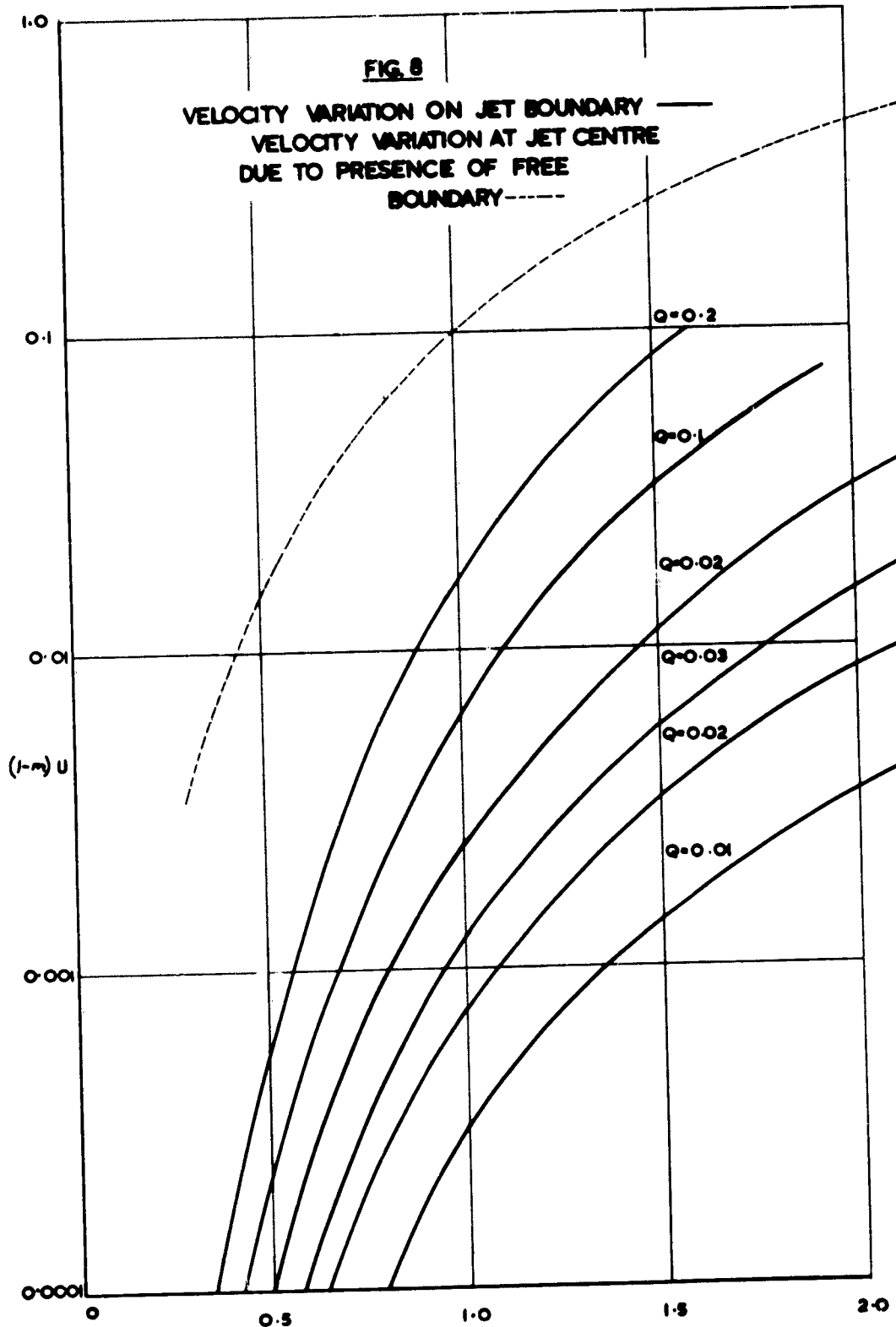


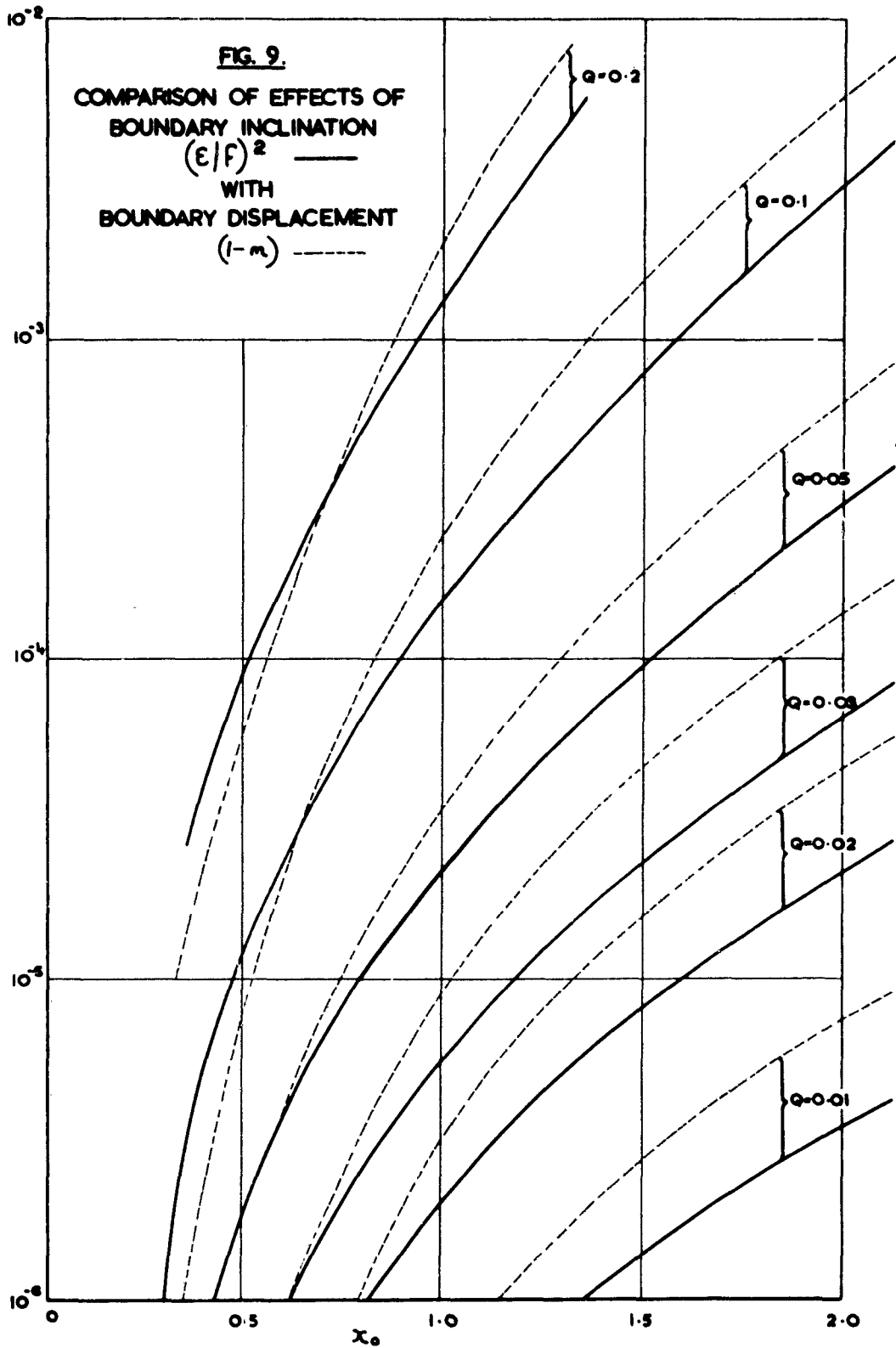
FIG. 6.
BOUNDARY EFFECT ON MODIFIED DRAG COEFFICIENT
OF AXISYMMETRIC CAVITY IN OPEN JET
(TWO DIMENSIONAL CASE SHOWN DASHED FOR COMPARISON.)

J

LF









*Information Centre
Knowledge Services*
[dstl] Porton Down,
Salisbury
Wiltshire
SP4 0JQ
22060-6218
Tel: 01980-613753
Fax 01980-613970

Defense Technical Information Center (DTIC)
8725 John J. Kingman Road, Suit 0944
Fort Belvoir, VA 22060-6218
U.S.A.

AD#: AD008775

Date of Search: 16 May 2008

Record Summary: DEFE 15/511

Title: Wall corrections to axially symmetric cavities in circular tunnels and jets
Availability Open Document, Open Description, Normal Closure before FOI Act: 30 years
Former reference (Department) Report No 7/52
Held by The National Archives, Kew

This document is now available at the National Archives, Kew, Surrey, United Kingdom.

DTIC has checked the National Archives Catalogue website (<http://www.nationalarchives.gov.uk>) and found the document is available and releasable to the public.

Access to UK public records is governed by statute, namely the Public Records Act, 1958, and the Public Records Act, 1967. The document has been released under the 30 year rule. (The vast majority of records selected for permanent preservation are made available to the public when they are 30 years old. This is commonly referred to as the 30 year rule and was established by the Public Records Act of 1967).

This document may be treated as UNLIMITED.